SMAR 2019 – Fifth Conference on Smart Monitoring,
Assessment and Rehabilitation of Civil Structures

SMAR 2019

A Coupled Damage-Plasticity Traction-Separation Law for Masonry

Yu Ping YUEN, Trisha DEB, Ku-Ming WANG, Yi-Cheng CHEN, Cheng-An TSAI, Wang-Wen CHEN

National Chiao Tung University, Hsinchu, Taiwan (Republic of China)

Contact e-mail: terryyyp@nctu.edu.tw

ABSTRACT: Due to the inherent brittleness, catastrophic collapse and damage of masonry structures can occur abruptly when the load-carrying capacity is exceeded. Failure of masonry structures in earthquakes and other extreme loading has been a major concern for the structural designers. Robust design of the structure relies on the accuracy of the structural response analysis under different loading conditions. Macroscopic strut-and-tie models and simplified continuum models are often used but they may not be able to simulate the detailed structural damage and the progressive collapse of the masonry structures. To this regards, a new and robust interfacial constitutive law, which couples the damage and plastic deformation with fracture energy-based softening rules, has been developed for the discrete finite element modelling (DFEM) of masonry structures. The model has 14 required parameters and the proposed model can successfully simulate a variety of mechanical behaviour of masonry structures including the pressure-dependent strength and fracture, wearing-off of the friction, dilatation behaviour, stiffness degradation, shear retention, and disintegration of the components. Several experiments on the masonry were simulated and good agreements between the simulated and experimental results could be observed. Comparing to the conventional microscopic models, the DFEM with the coupled damage-plasticity interfacial constitutive law can significantly simply the meshing work and the control of the mesh quality. Hence, the proposed model can be a practical tool for reliable failure and collapse analysis of masonry structures.

1 INTRODUCTION

A large number of existing residential, as well as historical buildings around the world, comprises of unreinforced masonry. Many of these structures are located on high seismic zones and have subsequently been affected by earthquake resulting in huge destruction (Zhang et al. 2017). The collapse of masonry structures during earthquakes and other extreme loading can jeopardize the structural safety and pose a grave threat to the occupants and property. Accurate and reliable analysis of the load-deformation behaviour of masonry under different types of loading is inarguably the most crucial step to guarantee a robust design of the masonry structures or buildings with masonry infill panels.

To this regard, this paper presents a new coupled damage-plasticity traction-separation law which is to be used with discrete finite element modelling (DFEM) of masonry structures which is able to simulate the structural collapse due to the disintegration of the components. The proposed model can simulate a variety of mechanical behaviour of masonry structures including the pressure-dependent strength and fracture, wearing off of the friction, dilation behaviour, stiffness degradation, shear retention, the disintegration of the components under different types of loading.

The calibration methods of all model parameters using common test data and physical rules are also provided in details. Simulations of various tests on masonry joints and a real scale masonry structure were then performed to validate the model performances.

2 MODEL DEVELOPMENT

2.1 Traction-separation law

An emerging novel modelling approach of masonry structures is the use of contact-interaction with discrete finite element modelling (DFEM) as illustrated in Figure 1. In DFEM, the masonry units are treated as individual deformable bodies, i.e. discrete elements that can be separated by a finite gap. The meshes of the masonry units are not necessary to be connected. No interfacial elements exist between the masonry units to model the mortar joints and the mechanic responses of the mortar joints are modelled as the interaction between the masonry units using the interfacial contact law. The general three-dimensional traction-separation law for the interfacical interaction reads as follows:

$$\begin{bmatrix}\sigma_n\\ \tau_1\\ \tau_2\end{bmatrix}=\begin{bmatrix}k_n & 0 & 0\\ 0 & k_{s1} & 0\\ 0 & 0 & k_{s2}\end{bmatrix}\begin{bmatrix}\delta_n^e\\ \delta_{s1}^e\\ \delta_{s2}^e\end{bmatrix} \text{ or } \boldsymbol{\sigma}=\mathbf{k_e}\cdot\boldsymbol{\delta}^e \tag{1}$$

where $\boldsymbol{\delta}^e=\boldsymbol{\delta}-\boldsymbol{\delta}^p$ is the elastic displacement of the total displacement vector $\boldsymbol{\delta}$ in which $\boldsymbol{\delta}^p$ is the plastic displacement; $\boldsymbol{\sigma}$ is the traction vector of the normal traction σ_n (corresponding to the normal displacement d_n^e) and the shear tractions in two perpendicular horizontal directions τ_1 and τ_2 (corresponding to the shear displacements s_1^e and s_2^e respectively); $\mathbf{k_e}$ is the effective elastic stiffness matrix.

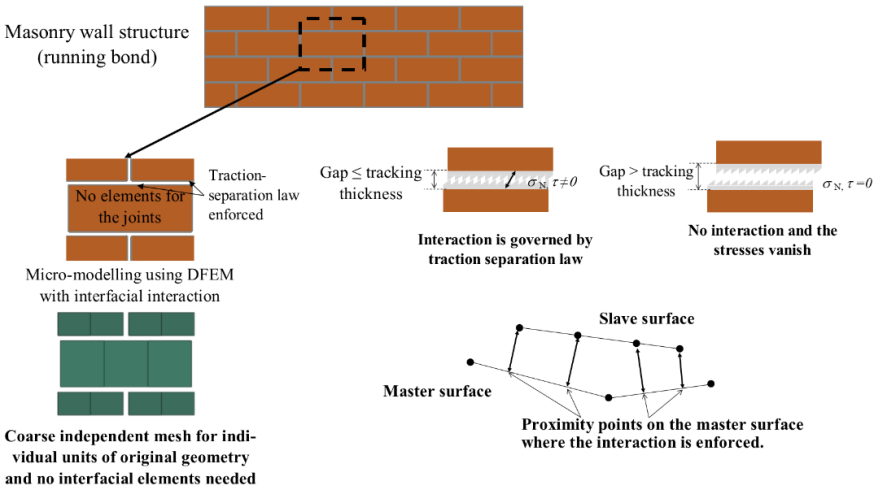

Figure 1. Discrete finite element modelling of masonry structures.

2.2 Inelastic deformation

Masonry walls are normally under vertical compression due to the self-weight and overburden loads. Horizontal loads such as earthquake and wind induce lateral shear and bending, which combine with the vertical compression to cause various stress states in different locations of the

walls. Hence, shear cracking caused by the combined shear and compressive stresses or flexural cracking caused by the tensile stress can be observed in the damaged masonry walls. The combined Mohr-Coulomb and tension-cut-off criteria are commonly used for modelling such fracture behaviour. Yet, the non-smooth intersections of the two criteria are not differentiable that can cause problems in computing the plastic flow numerically. A hyperbolic surface that is continuous and differentiable everywhere can approximate the combined Mohr-Coulomb and tension cut-off surface (Lotfi and Benson 1994). The hyperbolic yield surface for the mortar joint interfaces can be expressed as

$$F = \sqrt{\alpha^2 + \tau_1^2 + \tau_2^2} + \sigma_n \tan\phi - \beta = 0 \tag{2}$$

where $\tan\phi$, resembling the friction coefficient in the Mohr-Coulomb criterion, is the slope of the asymptotes of the hyperbolic surface; variables α and β can be correlated to the tensile resistance $\sigma_n = f_t$ when $\tau_1 = \tau_2 = 0$ and the shear cohesion $\tau_1^2 + \tau_2^2 = c^2$ when $\sigma_n = 0$ by using Eq. (2)

$$c = \sqrt{\beta^2 - \alpha^2}; \quad f_t = \frac{\beta - \alpha}{\tan\phi} \tag{3}$$

Hence, the evolution of the yield surface of Eq. (4) is controlled by internal variables ϕ, c, and f_t. It can be noted from Eq. (3) that the shear cohesion and tensile resistance are exhausted (i.e. $c = f_t = 0$) at the instant when $\alpha = \beta = 0$. Afterward, the plastic dissipation of the mortar is only governed by the friction process depending on the friction coefficient $\tan\phi$. Based on the assumptions by Lotfi and Shing (1994) the tensile softening rule by Stankowski (1992), the plastic-work softening rules can be applied for the internal variables as

$$f_t = f_{t0}\left(1 - \frac{w_I}{G_{IC}} - \frac{w_{II}}{G_{IIC}}\right) \geq 0 \tag{4}$$

$$c = c_{t0}\left(1 - \frac{w_I}{G_{IC}} - \frac{w_{II}}{G_{IIC}}\right) \geq 0 \tag{5}$$

$$tan\,\phi = tan\,\phi_r + (tan\,\phi_0 - tan\,\phi_r)e^{-m w_{III}} \tag{6}$$

where f_{t0} and c_{t0} are the initial tensile resistance and shear cohesion respectively; ϕ_0 and ϕ_r are the initial and residual friction angles respectively. G_{IC} and G_{IIC} are the mode I and mode II fracture energy respectively. m is a model constant. Inelastic work variables w_I, w_{II}, and w_{III} are defined as

$$w_I = \int \langle \sigma_n \rangle \dot{\delta}_n^{in} dt \tag{7}$$

$$w_{II} = \int (|\tau| - \langle -\sigma_n \rangle tan\,\phi)\, \dot{\delta}_s^{in} dt \tag{8}$$

$$w_{III} = \int \langle -\sigma_n \rangle |tan\,\phi - tan\,\phi_r|\, \dot{\delta}_s^{in} dt \tag{9}$$

in which δ_n^{in} is the total inelastic normal displacement, $|\tau| = \sqrt{\tau_1^2 + \tau_2^2}$ and $\delta_s^{in} = \sqrt{\left(\delta_{s1}^{in}\right)^2 + \left(\delta_{s2}^{in}\right)^2}$ are the resultant shear stress and total inelastic shear displacement respectively; $\langle\cdot\rangle$ is the Macauley brackets defined as $\langle A \rangle = (A + |A|)/2$. Eqs. (7) and (8) are the energy dissipations related to the mode I and mode II fractures. Eq. (9) is the energy dissipation due to the degradation of the friction coefficient. The total inelastic displacement $\boldsymbol{\delta}^{in}$ comprises the plastic displacement $\boldsymbol{\delta}^{p}$ and the crack opening/sliding $\boldsymbol{\delta}^{cr}$, i.e. $\boldsymbol{\delta}^{in} = \boldsymbol{\delta}^{p} + \boldsymbol{\delta}^{cr}$.

For frictional materials, non-associated flow rule, i.e. the plastic flow direction is not normal to the yield surface, often assumed to avoid excessive plastic dilation (plastic volume strain induced

by plastic shear strain). To model this plastic deformation behaviour, the following flow rule is assumed:

$$G = \sqrt{\tau_1^2 + \tau_2^2} + \sigma_n \tan\psi = 0 \tag{10}$$

The evolution of the dilation angle ψ in Eq. (10) is taken as the same as that of the friction angle (Eq. (6)) with a different constant n controlling the decay rate.

2.3 Stiffness degradation

The macroscopic stiffness of the mortar joints will be degraded with the increase of the crack opening and the accumulated inelastic deformation. This is due to the reduction of the contact area of the asperities or effective loading area which can be characterised by damage variables d. Then, to model the stiffness degradation behaviour, the concept of effective stress $\overline{\boldsymbol{\sigma}}$ in damage mechanics (Voyiadjis and Kattan 2005) can be used

$$\overline{\boldsymbol{\sigma}} = \boldsymbol{M}(d) \cdot \boldsymbol{\sigma} \tag{11}$$

where $\boldsymbol{\sigma}$ is the Cauchy stress tensor; $\mathbf{M}$ is the second-order damage effective tensor. While the mechanic behaviour of the undamaged part of the material may be still described by the yield criterion Eq.(2) and the plastic flow potential Eq.(10) presented in the last section but with the stress (traction) vector replaced by the effect stress (traction) vector $\overline{\boldsymbol{\sigma}}$, the damage part is assumed stress-free. Based on the hypothesis of strain equivalence, the effective elastic stiffness $\mathbf{k}_e$ in Eq. (1) can be defined as

$$\boldsymbol{k_e} = \boldsymbol{M}(d) \cdot \overline{\boldsymbol{k}}_{\boldsymbol{e}} \cdot \boldsymbol{M}(d) \tag{12}$$

in which $\overline{\mathbf{k}}_{\boldsymbol{e}}$ is the initial stiffness of the undamaged mortar joints. To model the stiffness degradation of the mortar joints, the damage tensor $\mathbf{M}$ is assumed as

$$\boldsymbol{M}(d) = \begin{bmatrix} \left(1 - d_n H(\sigma_n)\right)^{1/2} & 0 & 0 \\ 0 & \left(1 - d_s H(\sigma_n)\right)^{1/2} & 0 \\ 0 & 0 & \left(1 - d_s H(\sigma_n)\right)^{1/2} \end{bmatrix} \tag{13}$$

where d_n and d_s are the damage variables with values within [0, 1] corresponding to the normal and tangential (shear) stiffness receptively. The factor $(1 - d_s)$ is analogous to the classic shear retention factor used for modelling the shear stiffness degradation of fractured brittle materials (Chen 1982). $\mathrm{H}(\sigma_n) = 1$ for $\sigma_n > 0$ and $\mathrm{H}(\sigma_n) = 0$ for $\sigma_n \leq 0$, which is used to account for the unilateral effect (stiffness recovery) upon the crack closure. A linear transformation between the crack opening and the equivalent plastic displacement, $\delta^p = \sqrt{{\delta_n^p}^2 + {\delta_{s1}^p}^2 + {\delta_{s2}^p}^2}$, is assumed as follows:

$$\dot{\boldsymbol{\delta}}^{\boldsymbol{cr}} = \boldsymbol{b} \cdot \dot{\boldsymbol{\delta}}^{\boldsymbol{p}} \bar{\boldsymbol{\iota}} \tag{14}$$

where $\mathbf{b} = \mathrm{diag}[b_n \quad b_s \quad b_s]$ is a diagonal matrix of constant parameters and $\bar{\boldsymbol{\iota}} = [d\delta_n \quad d\delta_{s1} \quad d\delta_{s2}]^{\mathrm{T}} / |\dot{\delta}|$ is the unit direction vector of the displacement increment. The relationships among the effective elastic displacement $\overline{\boldsymbol{\delta}}^{\boldsymbol{e}}$, plastic displacement $\boldsymbol{\delta}^{\boldsymbol{p}}$, and crack opening $\boldsymbol{\delta}^{\boldsymbol{cr}}$, the damage tensor $\mathbf{M}(d)$ can be correlated to the plastic and the total displacement by

$$\boldsymbol{I} - \boldsymbol{M}^{\boldsymbol{2}} = \boldsymbol{b} \cdot \boldsymbol{\delta}^{\boldsymbol{p}} \cdot (\boldsymbol{\delta} - \boldsymbol{\delta}^{\boldsymbol{p}})^{-\boldsymbol{1}} \tag{15}$$

in which **I** is the identity matrix**.**

2.4 Incremental form

To implement the coupled damage-plasticity traction-separation model in general FE codes, an incremental form of the constitutive relationship shall be established. The incremental form of Eq. (1) can be rewritten as

$$\boldsymbol{\Delta\sigma} = \boldsymbol{k_e} \cdot (\boldsymbol{\Delta\delta} - \boldsymbol{\Delta\delta^p}) + \boldsymbol{\delta^e} \cdot \left(\frac{\partial \boldsymbol{k_e}}{\partial \boldsymbol{d^p}} \cdot \boldsymbol{\Delta\delta^p}\right) \tag{16}$$

The plastic displacement increment and the crack displacement increment are

$$\boldsymbol{\Delta\delta^p} = \boldsymbol{\Delta\lambda}\frac{\partial \boldsymbol{G}}{\partial \boldsymbol{\sigma}};\ \boldsymbol{\Delta\delta^{cr}} = \boldsymbol{\Delta\lambda b} \cdot \frac{\partial \boldsymbol{G}}{\partial \boldsymbol{\sigma}} \tag{17}$$

The plastic multiplier increment $\Delta\lambda$ is determined by the consistency condition. Hence, the plastic displacement increment can be expressed as

$$\boldsymbol{\Delta\delta^p} = \left(\frac{(\partial \boldsymbol{F}/\partial \boldsymbol{\sigma})\cdot \boldsymbol{k_e}\cdot \boldsymbol{\Delta\delta}}{\boldsymbol{H'} + (\partial \boldsymbol{F}/\partial \boldsymbol{\sigma})\cdot \boldsymbol{k_e}\cdot(\partial \boldsymbol{G}/\partial \boldsymbol{\sigma})}\right)\frac{\partial \boldsymbol{G}}{\partial \boldsymbol{\sigma}} \tag{18}$$

in which H' is the effective plastic modulus given by

$$\boldsymbol{H'} = -\frac{\partial \boldsymbol{F}}{\partial \boldsymbol{\xi}} \cdot \frac{\partial \boldsymbol{\xi}}{\partial \boldsymbol{d^p}} \cdot \frac{\partial \boldsymbol{G}}{\partial \boldsymbol{\sigma}} - \frac{\partial \boldsymbol{F}}{\partial \boldsymbol{\sigma}} \cdot \left(\frac{\partial \boldsymbol{k_e}}{\partial \boldsymbol{\delta^p}} \cdot \frac{\partial \boldsymbol{G}}{\partial \boldsymbol{\sigma}}\right) \cdot \boldsymbol{\delta^e} \tag{19}$$

The first term is the classic plastic modulus due to the hardening/softening of the yield surface and the second term is due to the degradation of the effective elastic stiffness $\mathbf{k}_e$. $H' < 0$ for softening materials, $H' > 0$ for hardening materials, $H' = 0$ for perfect yielding materials. Then, the relationship between the traction increment and total separation increment can be obtained:

$$\boldsymbol{\Delta\sigma_i} = \left[\boldsymbol{k_e} - \frac{\left(\boldsymbol{k_e}\cdot\frac{\partial \boldsymbol{G}}{\partial \boldsymbol{\sigma}}\right)\otimes\left(\frac{\partial \boldsymbol{F}}{\partial \boldsymbol{\sigma}}\cdot \boldsymbol{k_e}\right)}{\boldsymbol{H'} + \frac{\partial \boldsymbol{F}}{\partial \boldsymbol{\sigma}}\cdot \boldsymbol{k_e}\cdot\frac{\partial \boldsymbol{G}}{\partial \boldsymbol{\sigma}}} + \frac{\left(\boldsymbol{\delta^e}\cdot\frac{\partial \boldsymbol{k_e}}{\partial \boldsymbol{d^p}}\cdot\frac{\partial \boldsymbol{G}}{\partial \boldsymbol{\sigma}}\right)\otimes\left(\frac{\partial \boldsymbol{F}}{\partial \boldsymbol{\sigma}}\cdot \boldsymbol{k_e}\right)}{\boldsymbol{H'} + \frac{\partial \boldsymbol{F}}{\partial \boldsymbol{\sigma}}\cdot \boldsymbol{k_e}\cdot\frac{\partial \boldsymbol{G}}{\partial \boldsymbol{\sigma}}}\right] \cdot \boldsymbol{\Delta\delta} = \boldsymbol{k_{ep}} \cdot \boldsymbol{\Delta\delta} \tag{20}$$

where $\mathbf{k}_{\text{ep}} = \mathbf{k}_e + \mathbf{k}_p + \mathbf{k}_d$ is the elastoplastic tangential stiffness matrix which is the linear combination of the effective elastic stiffness $\mathbf{k}_e$, the plastic stiffness matrix $\mathbf{k}_p$, and the coupled damage-plastic stiffness matrix $\mathbf{k}_d$ defined as:

$$\boldsymbol{k_e} = \begin{bmatrix} \boldsymbol{k_n}(\boldsymbol{1} - \boldsymbol{d_n}\boldsymbol{H}(\boldsymbol{\sigma_n})) & \boldsymbol{0} & \boldsymbol{0} \\ \boldsymbol{0} & \boldsymbol{k_{t1}}(\boldsymbol{1} - \boldsymbol{d_s}\boldsymbol{H}(\boldsymbol{\sigma_n})) & \boldsymbol{0} \\ \boldsymbol{0} & \boldsymbol{0} & \boldsymbol{k_{t2}}(\boldsymbol{1} - \boldsymbol{d_s}\boldsymbol{H}(\boldsymbol{\sigma_n})) \end{bmatrix} \tag{21}$$

$$\boldsymbol{k_p} = -\frac{\left(\boldsymbol{k_e}\cdot\frac{\partial \boldsymbol{G}}{\partial \boldsymbol{\sigma}}\right)\otimes\left(\frac{\partial \boldsymbol{F}}{\partial \boldsymbol{\sigma}}\cdot \boldsymbol{k_e}\right)}{\boldsymbol{H'} + \frac{\partial \boldsymbol{F}}{\partial \boldsymbol{\sigma}}\cdot \boldsymbol{k_e}\cdot\frac{\partial \boldsymbol{G}}{\partial \boldsymbol{\sigma}}} \tag{22}$$

$$\boldsymbol{k_d} = \frac{\left(\boldsymbol{\delta^e}\cdot\frac{\partial \boldsymbol{k_e}}{\partial \boldsymbol{d^p}}\cdot\frac{\partial \boldsymbol{G}}{\partial \boldsymbol{\sigma}}\right)\otimes\left(\frac{\partial \boldsymbol{F}}{\partial \boldsymbol{\sigma}}\cdot \boldsymbol{k_e}\right)}{\boldsymbol{H'} + \frac{\partial \boldsymbol{F}}{\partial \boldsymbol{\sigma}}\cdot \boldsymbol{k_e}\cdot\frac{\partial \boldsymbol{G}}{\partial \boldsymbol{\sigma}}} \tag{23}$$

The proposed coupled damage-plasticity traction separation law was implemented in ABAQUS using user-subroutine VUINTERACTION (ABAQUS Inc. 2014) which is used with the general contact interaction of the mortar joint interfaces. For time step i, each nodal point of the contacting surface is provided with the displacement increment $\Delta\boldsymbol{\delta}_i$ and the previous state and internal variables i.e. $\boldsymbol{\xi}_i$, $\boldsymbol{\delta}_i^{cr}$, and $\boldsymbol{\delta}_i^{p}$. Then, the incremental traction separation law Eq. (20) are numerically integrated using the modified explicit Euler scheme with sub-stepping (Sloan et al. 2001).

3 MODEL VALIDATION

3.1 Shear tests

All 14 required parameters of the proposed traction-separation law with coupled damage-plastic models are summarised in Table 1. Many of the model parameters, i.e. the stiffness $\bar{k}_n$ and $\bar{k}_{si}$, the tensile and shear strengths f_{t0} and c_{t0}, the friction and dilation angles ϕ_0 and ψ_0 can be directly obtained from standard tensile and shear-compression strength tests or empirical/analytical relationships for specific types of masonry. The monotonic shear tests on JG bricks with type B mortar reported by van der Pluijm (1993) are simulated with the proposed model. The model parameters summarized in Table 1. The experiment results and the simulated shear stress-displacement curves are plotted together in Figure 2. Good agreements between the simulated and the experimental behaviour can be observed. The pressure-dependent shear stress-displacement behaviour can be well simulated by the proposed model. It is noted that the pressure-dependent mode II fracture energy as reported by van der Pluijm (1993) was adopted in the simulation. The cyclic shear test on clay bricks with 13 mm mortar joint thickness reported by Atkinson et al. (1988) are then simulated (Figure 3). The resulted cyclic shear stress-displacement behaviour with degradation of the friction angle leads to the hysteretic loops slowly varying during the loading cycles which can match the experiment results.

Table 1. Values of the model parameters for the simulations of different tests.

Parameters	Monotonic shear tests (van der Pluijm 1993)	Cyclic shear tests (Atkinson et al. 1988)	Uniaxial tension tests (Almeida et al. 2002)
$\bar{k}_n$ (MPa/mm)	209.9	471.4	741.1, 750.5[b]
$\bar{k}_{si}$ (MPa/mm)	87.4	196.4	308.8, 312.7 [b]
f_{t0} (MPa)	0.62	0.085	1.78, 0.91
c_0 (MPa)	0.88	0.128	2.67, 1.37
G_{IC} (N/mm)	0.00458	0.0242	0.01209, 0.00293 [b]
G_{IIC} (N/mm)	0.058	0.1933	0.121, 0.02925 [b]
ϕ_0 (degree)	40.97	35.26	40
ϕ_r (degree)	36.87	34.72	32
m (mm)	10547.4, 1217.7, 398.3[a]	50.4	511.9, 2944.5 [b]
ψ_0 (degree)	27.7	0.544	8
ψ_r (degree)	0	0	0
n (mm)	15836.0, 1828.3, 598.1[a]	367.96	856.1, 4923.8 [b]
b_n	10	10	10
b_s	3	3	3

[a]Parameter values $\sigma_n = -0.1, -0.5, -1.0$ MPa. [b]For $\sigma_n = -0.1, -0.5, -1.0$ MPa. [b]Parameter values for 1:3 mortar and 1:2:9 mortar respectively.

3.2 Tensile tests

The tensile properties of masonry units and mortar determined by standard uniaxial tension tests are relatively stable, while the tensile bonding strength between the units and mortar joints often shows signification variation that can be influenced by the test methods and the preparation procedures Almeida et al. (2002). Nevertheless, the traction-separation relationship should be able to properly model the bonding behaviour of the masonry units and the mortar joints, which can dictate the global force-deformation behaviour of the masonry structures. The uniaxial tension test on solid ceramic bricks with 1:3 (cement: sand) mortar (test M15) and 1:2:9 (cement: lime: sand) mortar (test M34) reported by Almeida et al. (2002) are simulated by the proposed modelling. The model parameters are summarised in Table1. As shown in Figure 4, the simulated

tension stress-displacement curves agree well with the experimental results. But it should be emphasised that the tensile bonding behaviour of the masonry joints can show significant variations depending on the workmanship. Hence, for practical design, the conservative values of the tensile strength and the mode I fracture energy shall be adopted.

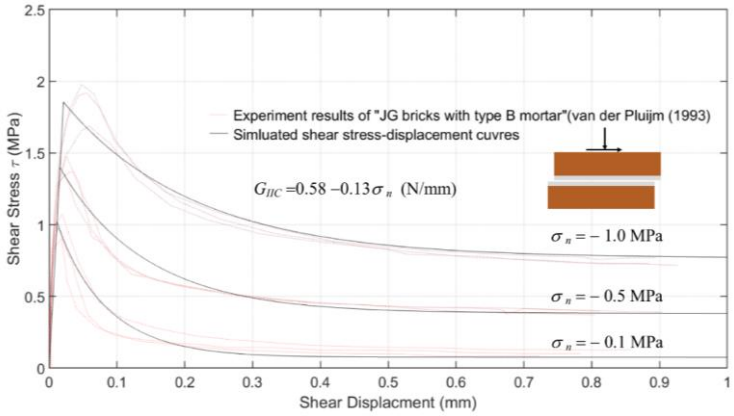

Figure 2. Experimental (Van derPluijm 1993) and simulated monotonic shear stress-displacement curves under different levels of normal compression.

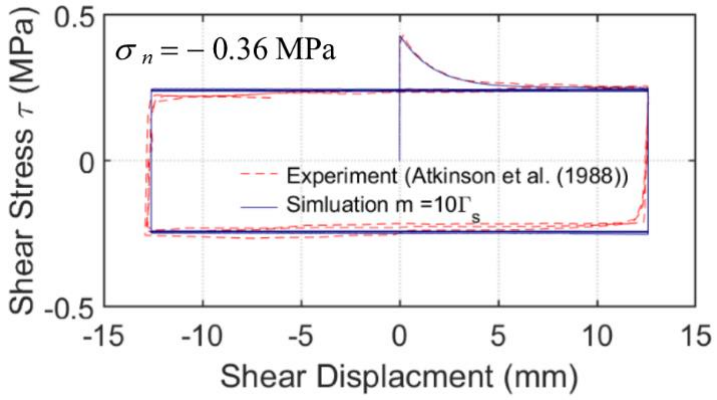

Figure 3. Experimental (Atkinson et al. 1988) and simulated cyclic shear stress-displacement curves.

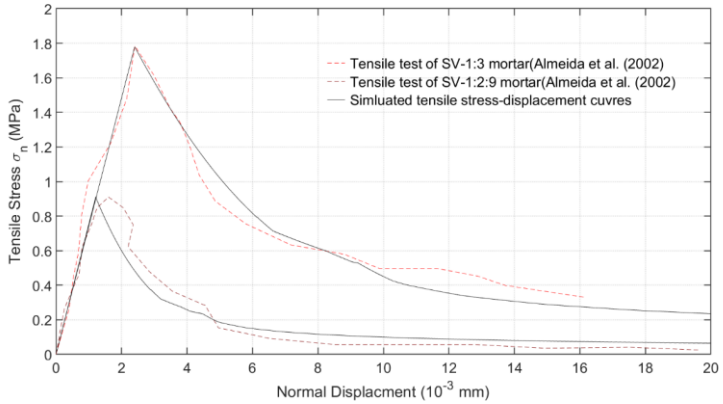

Figure 4. Experimental (Almeida et al. 2002) and simulated tensile stress-displacement curves.

4 CONCLUSIONS

A new and rigorous coupled damage-plasticity traction-separation law was successfully developed and implemented for discrete finite element modelling (DFEM) to simulate the inelastic deformation and failure of masonry structures. By proper calibration of the model parameters, a variety of mechanical behaviour of masonry structures can be accurately modelled including (1) the pressure-dependent friction and shear fracture behaviour, (2) the strength softening with inelastic work, (3) evolution of the friction angle, (4) the pressure-dependent dilation, (5) stiffness degradation due to the crack opening, (6) shear retention, and (7) disintegration of the masonry units.

The proposed model was applied to simulate shear-compression tests, cyclic shear tests, and tension tests on the masonry joints. Following the suggested calibration methods, the simulated results agree well with the experimental results. Given its flexibility in modelling a range of mechanical behaviour and validated performances, the proposed model can be adopted for the detail and reliable analysis of the responses of masonry structures under different types of loading.

5 ACKNOWLEDGMENTS

The support of the Ministry of Science and Technology (MOST), R.O.C. under Grand Numbers 107-2636-E-009-002- and 108-2636-E-009 -005- are gratefully acknowledged.

6 REFERENCES

ABAQUS Inc. 2014. *Abaqus User Subroutines Reference Guide*.

Almeida, JC, Lourenço, PB, and Barros, JA, 2002, Characterization of brick and brick-mortar interface under uniaxial tension. *The VII International Seminar on Structural Masonry for Developing Countries*. Belo Horizonte, Brasil.

Atkinson, RH, Kingsley, GR, Saeb, S, et al, 1988, A laboratory and in situ study of the shear strength of masonry bed joints. *Proceedings of the Eighth International Brick and Block Masonry Conference*. Dublin, Ireland, pp 261–271.

Chen, WF. 1982. *Plasticity in Reinforced Concrete*. McGraw-Hill, New York.

Lotfi, HR, and Benson, SP, 1994, Interface Model Applied to Fracture of Masonry Structures. *Journal of Structural Engineering*, 120:63–80.

Sloan, SW, Abbo, AJ, and Sheng, D, 2001, Refined explicit integration of elastoplastic models with automatic error control. *Engineering Computations*, 18:121–194.

Stankowski, T, 1992, Numerical simulation of failure in particle composites. *Computers & Structures*, 44:459–468.

van der Pluijm, R, 1993, Shear behaviour of bed joints. *Proceedings of the 6th North American Masonry Conference*, Philadelphia, USA, 6-9 june. pp 125–136.

Voyiadjis, GZ, and Kattan, PI, 2005, *Damage Mechanics*, 1st edn. CRC Press, Boca Raton.

Zhang, H, Kuang, JS, and Yuen, TYP, 2017, Low-seismic damage strategies for infilled RC frames: shake-table tests. *Earthquake Engineering & Structural Dynamics*, 46:2419–2438.